Arch. Metall. Mater. **69** (2024), 2, 795-801

DOI: https://doi.org/10.24425/amm.2024.149812

R. HARAGA[1], D. CHICET[1*], S. TOMA[1], V. CARLESCU[2], C. BEJINARIU[1]

MICROHARDNESS AND ELASTIC PROPERTIES EVALUATION OF WC-TiC COATINGS OBTAINED BY ARC SPRAYING PROCESS

Fulfilling the basic role of hard thermal sprayied coatings is closely related to the value of its microhardness. The quality of such a layer depends on several variables, the main categories being: spray method (flame spray, electric arc, plasma spray, cold spray, etc.), spray parameters (spray distance, voltage and intensity, working atmosphere, direction of the spray jet, etc.) and the materials used (chemical composition of the coating materials, quality and texture of the substrate). In this study, the microhardness, elastic properties and cohesion of a coating made of hard cored wire (Praxair – Tafa) by electric arc spraying process on a low alloy steel substrate, were analyzed. The cored wire has as main hard elements WC (about 26%) and TiC (about 6%), the rest of the chemical elements present being: Cr (14%), Ni (4.5%), B (1.87%), Si (1.25%) and the Fe balance. The micro-hardness was evaluated onto the surface of the coating, previously prepared by grinding to reduce the as-coated roughness. The method based on recording the forcess generated during the indentation with simultaneous measurement of the load – depth curve (with UMT 2M-CETR microtribometer) were used for the microhardness evaluation. In order to analyse the cohesion of the coated layer, scratch tests with progressive loading (10N, 15N and 20N) were performed on the same microtribometer. Tests have shown that the metal matrix uniformly includes the hard particles arised from the core of the wire, and at the microstructural level, the microhardness varies significantly, depending on the hardness of the particles on which the indentor tip applies the loading forces. However, the overall behavior of the coatings thus realized is a satisfactory one, being, as a general behavior, in the average required by the applications of such a layer.

Keyword: Microhardness; Cored Wire; WC-TiC hard particles; Arc Spraying Process

1. Introduction

Coatings obtained by thermal spraying have been used for several decades to improve the characteristics of functional surfaces, among which can be mentioned: resistance to sliding wear [1], abrasive wear [2], contact fatigue [3], corrosion [4], high temperatures [5], thermal insulation or biocompatibility [6].

Obtaining coatings with various applications depends primarily on the type of materials used, which can be metals, alloys or mixtures (based on Fe, Ni or Co), carbides (WC/W2C, WTiC, Cr_2C_3 with matrix of Fe, Ni or Co for applications that require wear resistance in difficult environments), ceramic oxides (oxides of Al, Cr, Zr, Ti, Y simple or in various combinations), MCrAlY for applications at high temperatures in corrosive environments or cermets (e.g. $NiAl_2O_3$) which combines the two materials and are generally used as an intermediate layer to take over the differences in thermal expansion between two different layers [7].

The second major influence is that given by the deposition technology, the thermal coatings can be made by several methods: flame spray (FS) [8], high-velocity-oxy-fuel (HVOF) [9], electric arc spraying (EAS) [10], cold spray (CS) [11], atmospheric plasma spray (APS) [12] or their variants, each bringing with it various changes in the characteristics of the coatings made (density, porosity, structural homogeneity, adhesion to the substrate, cohesion, tribological or thermal characteristics, etc.).

One of the well-known and often used methods of thermal deposition is the electric arc (EAS), commonly called metallization. This is one of the cheapest methods of thermal deposition, whose working principle consists in the formation of an electric arc between the ends of two electrodes (wires fed through the deposition gun), reaching a temperature close to that of melting the material of the wires. In this way, a bath of molten metal is formed which is continuously atomized with the help of a gas under pressure and accelerated towards the substrate on which it will be successively deposited in the form of splashes [13].

[1] GHEORGHE ASACHI TECHNICAL UNIVERSITY OF IASI, DEPARTMENT OF MATERIALS SCIENCE AND ENGINEERING, BLVD. MANGERON, NO. 41, 700050, IASI, ROMANIA
[2] GHEORGHE ASACHI TECHNICAL UNIVERSITY OF IASI, DEPARTMENT OF MECHANICAL ENGINEERING, BLVD. MANGERON, NO. 61, 700050, IASI, ROMANIA

* Coressponding author: daniela-lucia.chicet@academic.tuiasi.ro

In addition to the compact wire usually used, this method can also use a special type of wire, which is produced in the form of a tube and contains inside hard reinforcing particles in the form of a core, being called cored wire [14]. This type of wire brings with it the advantage of introducing very hard particles into the metal matrix which is usually Ni or Fe [15], ensuring the formation of layers with superior properties through a method that is not as demanding and expensive as HVOF or APS.

Regarding the characterization of the coatings, the morphological evaluation based on the microstructural analysis by OM and SEM is used in research practice, supplemented by that of the chemical and phase composition by EDS or XRD. Additionally, for each targeted property, standardized and experimental methods for determining and comparative analysis of the obtained data are established, of interest for the present research being the elastic and microhardness properties. In the case of coatings deposited by thermal spraying, these properties are usually analyzed within the evaluation of their adhesion to the substrate or the analysis of the cohesion of the coating [16]. Thermal spray coatings have a heterogeneous layered structure. Determining the characteristics of these coatings is important because this can define their limits of use (static or dynamic stresses, wet or dry wear environments, and so on).

For these evaluations, multiple standardized methods are approached, based on [17]: bending and twisting, ball burnishing, chisel, extrusion, thermal shock, grinding and sawing (BS EN ISO 2819/1985), bend test (BS 5411), shearing (BS EN 2829), shot peening (BS EN 2830), impact with drop weight or push test (ASTM 13571), coating fixture with special adhesive (ASTM C633) a.s.o. Due to the continuous development of the applications of coatings deposited by thermal spraying, new methods of their evaluation and characterization are also being approached, two of them being the scratch test and the indentation test. These were initially applied only on thin layers and later found their applicability also for the characterization of thicker coatings such as those made by thermal spraying, being currently used both on a laboratory scale and in industrial practice.

The indentation test is based on the analysis of the response of the coating in the area of application, with a certain force, of an indenter, as a result of which elastic, plastic deformations, cracking or even delamination of the layer can be recorded in the tested area [18].

The scratch test is based on applying a diamond tip to the surface of the coating and pulling it in a certain linear direction, to obtain a scratch mark. This test can be applied both on the surface of the coating and on its cross-section (in which case the sample must be embedded in the resin support), with constant or progressive force, in one or more passes [19]. The way in which the tested surface is affected (plastic deformation, cracking or exfoliation) is correlated with the frictional forces recorded during the test in order to conclude on the critical loads at which the different mechanisms of destruction of the tested coating occur [20].

Acoustic emissions (AE) are deformation waves generated by the sudden redistribution of internal stresses in materials or structures, when changes occur in their internal structure [21-23]. The possible sources of AE can be: initiation and growth of cracks, deformation, dislocation movement, void formation, interfacial destruction, corrosion, debonding of matrix fibers in composite materials, etc. [24,25]. AE recording during scratch tests applied to layers with various compositions was introduced as an additional tool needed to accurately determine the causes of specific damages that are then attributed to critical loads that can generate layer destruction [26-28].

2. Experimental procedure

2.1. Materials and methods

In the present paper, the research was performed on one type of coating produced by electric arc spray, using a commercial hard cored wire (Praxair – Tafa) by electric arc spraying process on a C45 low alloy steel substrate (0.42-0.50% C, 0.4% Si, 0.50-0.80% Mn, max. 0.045% P, max. 0.045% S, 0.4% Cr, 0.1% Mo, 0.4% Ni). The cored wire has as main hard elements WC (about 26%) and TiC (about 6%), the rest of the chemical elements present being: Cr (14%), Ni (4.5%), B (1.87%), Si (1.25%) and the Fe balance. This type of coating contains an appreciable amount of ultra-hard particles and is used to replace hard chromium plating, which is intended to be replaced due to environmental risk.

The substrate was prepared in the form of a parallelepiped, with the size of 10×10×50 mm, and the preparation of the surface for thermal deposition was carried out according to the usual procedures: sandblasting and degreasing the surface with acetone. To ensure the best possible interpretation, three samples with WC-TiC coating were made and tested.

2.2. Samples characterisation

Several methods were used to analyze the microhardness and elastic characteristics of the coatings. The method based on recording the forcess generated during the indentation with simultaneous measurement of the load – depth curve was used for the microhardness evaluation. For this purpose, a universal material testing equipment was used: the UMT-2 CETR Tribometer (now Bruker) for measuring the mechanical and tribological properties of materials and coatings on the microscale. From construction point of view, the UMT-2 Tribometer consists of three modules, each moving in one direction/axis. Thus, at the top of the equipment is placed the carriage which moves in the vertical up-down direction or z-axis, representing the direction in which the load is applied. Attached to the trolley is the slider module which moves horizontally left-right in the x-axis direction and the linear mass module is placed at the bottom of the equipment and moves back and forth in the y-axis direction. The equipment allows the evaluation of the microhardness of materials or coatings by the indentation procedure with low loads, and in this study a Vickers indenter, square-base

pyramid with an angle at the tip of 130 was used, as presented in Fig. 1a.

The hardness is calculated automatically by the software of the equipment based on the values of the load and the penetration depth and not by measuring the diagonal marks left in the material after the indenter penetration as is the traditional method, because the equipment does not have an optical system to measure the size of the diagonals.

The indentation force (normal to the sample) is applied via the force sensor attached to the tribometer carriage and the penetration depth is determined using a capacitive sensor (0.05-250 μm) from MTI Instruments.

The pressing force Fz and penetration were recorded throughout the indentation procedure. The procedure sequences were:

– Preload with 10% of maximum force: 2 N for 5 s;
– Microindentation: increasing force over time (loading): from 2 N to 20 N for 30 s; constant force – holding at maximum force of 20 N for 15 s; decreasing force in time (unloading): from 20 N to 2 N for 30 s; constant force – holding at 2 N force for 15 s; complete discharge: from 2 N to 0.1 N for 5 s.

Following indentation, the Viewer software of the tribometer allowed the indentation force-depth of penetration curves to be highlighted and the microhardness to be determined automatically by analysing the slope of the discharge curve. For our tests at low loads and taking into account the time of maintenance of the maximum force, the hardness scale will be noted HV2/15.

The scratch test involves the application of a constant or time-varying pressure force to an indenter moving on the surface of a sample at a certain speed. This test can be applied to many materials such as thin films, fragile ceramics, coating layers, polymers, etc. The determination of the scratch properties of the coatings in this study was carried out using the same tribometer (UMT-2 CETR), the experimental configuration being presented in Fig. 1b. The samples were fixed on the linear table of the tribometer and the scratch test was performed using a blade with a tip radius of 0.4 mm fixed on an elastic adapter in the force sensor. The scratch test was performed at a variable force increasing over time, from 0.1 to 10 N (test 1), 15 N (test 2) and 20 N (test 3) over a distance of 10 mm at a speed of 0.167 mm /s. In addition to the friction coefficient specific to each test, another parameter measured during the scratch test was the acoustic emission (AE) that occurs as a result of the reaction of the coating to the application of the progressive force on the blade. The evaluation of the scratch resistance of the deposited layers was done by analyzing the variation graphs of the coefficient of friction (COF) when scratching.

In addition, the morphology of the surfaces of the tested coatings was analyzed, both by direct observation and with the help of electron microscopy, the Vega Tescan LMH2II electron microscope being used for this purpose.

Prior to applying the micro-indentation and scratch tests, the surfaces of the tested samples were sanded with 1000 grit sandpaper to reduce the specific asperities of the coatings obtained by thermal spraying. The roughness was determined using the Mitutoyo SJ-301 portable roughness meter, with a measurement medium speed of 0.5 mm/s. The average initial roughness of the coatings in the unprocessed state was 14.09 μm, and after grinding it became 6.07 μm.

3. Results and discussions

3.1. Thermal coatings characterisation

The morphology of the coatings was analyzed by electron microscopy both on the surface of the layer, as on the cross-section, as shown in Fig. 2. The specific appearance with splat-type particles can be observed, but also the presence of unmelted spherical particles, which have adhered to the surface of the coating. In terms of cross-sectional appearance, the average thickness of the coatings sprayied on the studied samples is about 600 μm, an example being the one shown in Fig. 2b, where a coating thickness of 618 μm is observed. On this image can also be seen the way of superposition of the splats of molten material (the metallic matrix), which includes the hard W or Ti carbide particles that are evenly distributed throughout the thickness of the layer.

The images in Fig. 3 show some aspects of the traces resulting from the scratch tests. Fig. 3a shows the appearance of

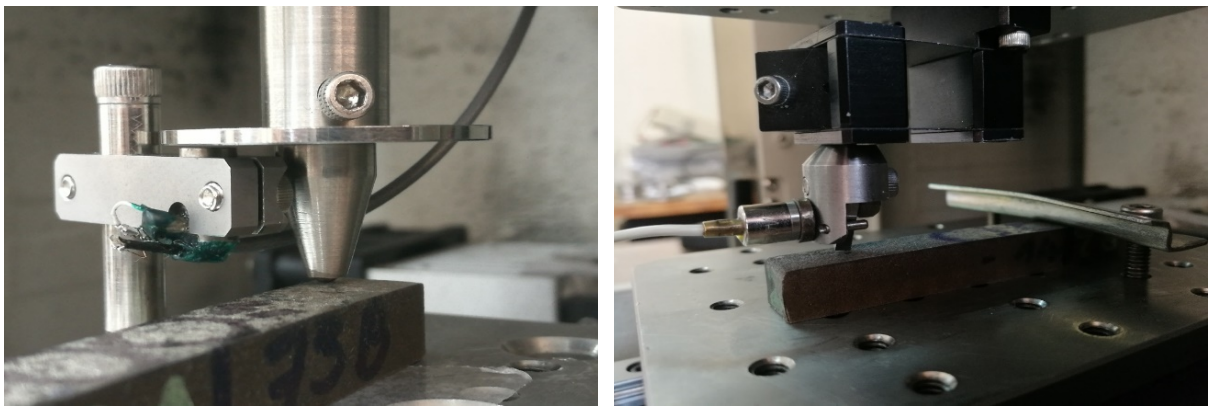

a) b)

Fig. 1. Test configurations by: a) microindentation; b) scratch

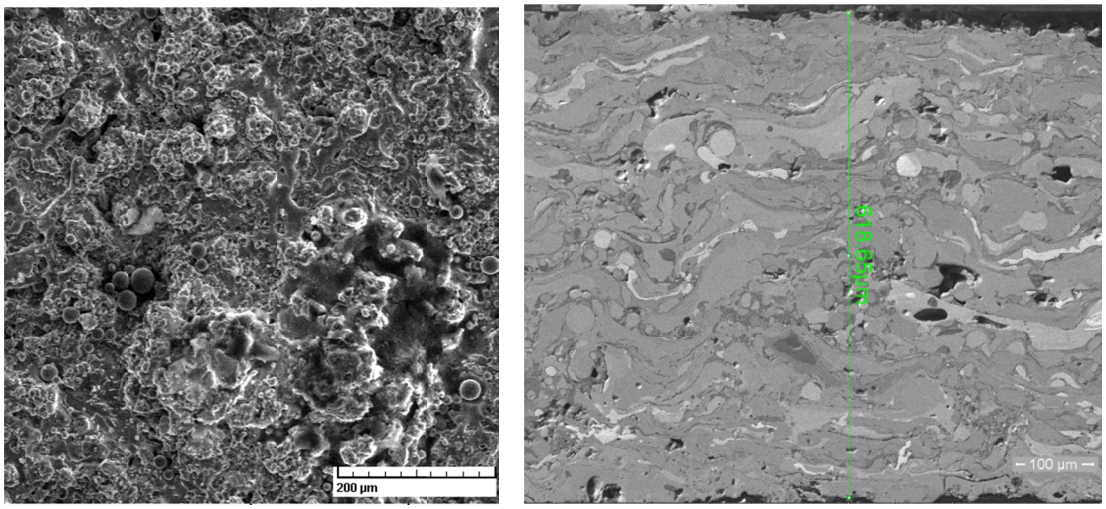

a) b)

Fig. 2. Secondary electron images of a) the as-coated surface and b) the section of one of the studied samples

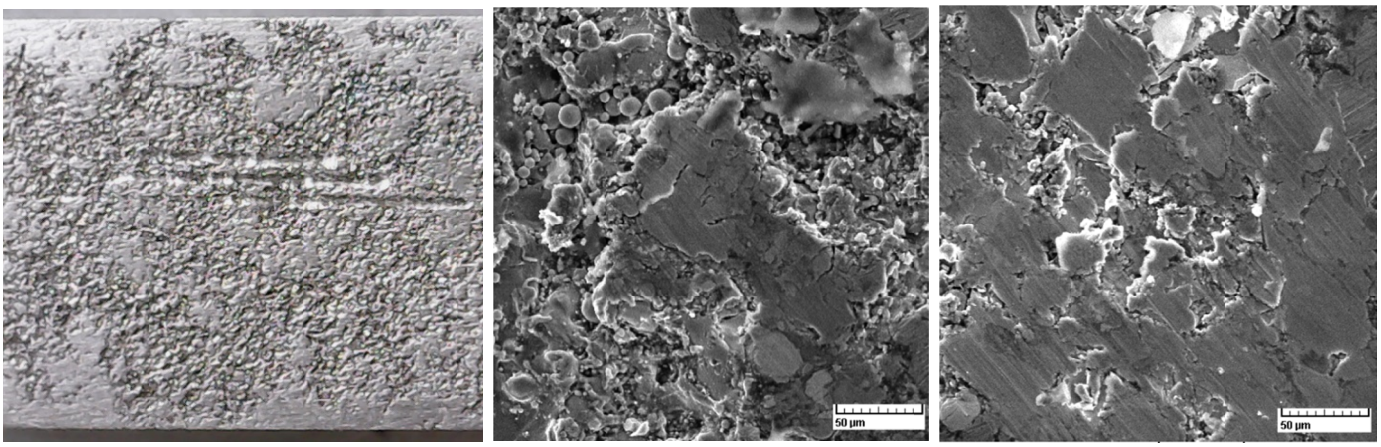

a) b) c)

Fig. 3. Analysis of the traces resulting from the scratch tests: a) 5× stereomicroscope image; b) image of secondary electrons on the scratch mark initiation area at 20 N; c) image of secondary electrons on the final area of the scratch mark at 20 N

the three traces generated at a distance of 1 mm between them, for each load of 10, 15 and 20 N (from bottom to top), shifted as a starting point by 2 mm. It can be seen that with each type of load, the starting point is blurred, after which the trace becomes more and more visible as the load increases. Figs. 3b and 3c show how the surface was affected by the scratch test, the majority being plastic deformation followed by exfoliation of the material that forms the coating.

3.2. Micro-indentation behaviour

The indentation tests were performed on the surface of the deposited layer, after bringing it to an average roughness of 6.07 µm, in several randomly chosen points on each sample.

As can be seen from the representative indentation graphs presented in Fig. 4, the behavior is different in the analyzed points, a specific aspect for such a coating made of washes, which contains a high percentage of hard particles from WC and TiC. The recorded microhardness values vary between 0.463 GPa and 0.908 GPa, the average value of the 20 measurements made being 0.7204 GPa.

3.3. Scratch tests results

The scratch tests were performed at different progressive loads, of 10, 15 and 20 N, in order to be able to perform a comparative evaluation of the response of the coating, both through the lens of how it is affected and through the lens of the friction coefficient recorded during the tests. Thus, it was observed that in all three cases the friction force (Ff) registered an increase directly proportional to the load, but this did not have a linear route but with peaks, the maximum values being observed in the last 20 seconds of the test. In the case of the scratch test at a load of 10 N, a value of about 4N was recorded in the 11th second, a bit of 7 N in the 20th second and a maximum of 11.2 N in the 55th second. In the case of the test at a load of 15 N, in the 11th

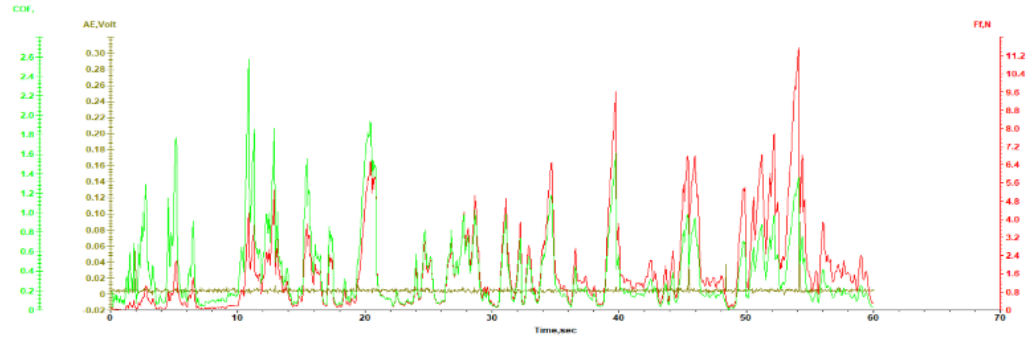

a)

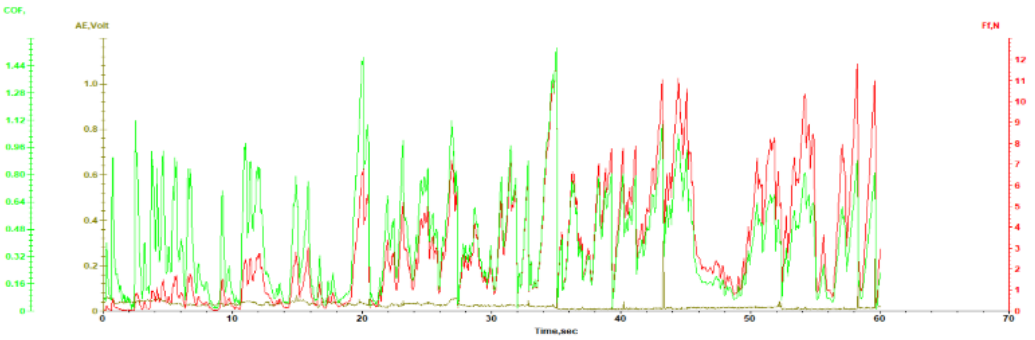

b)

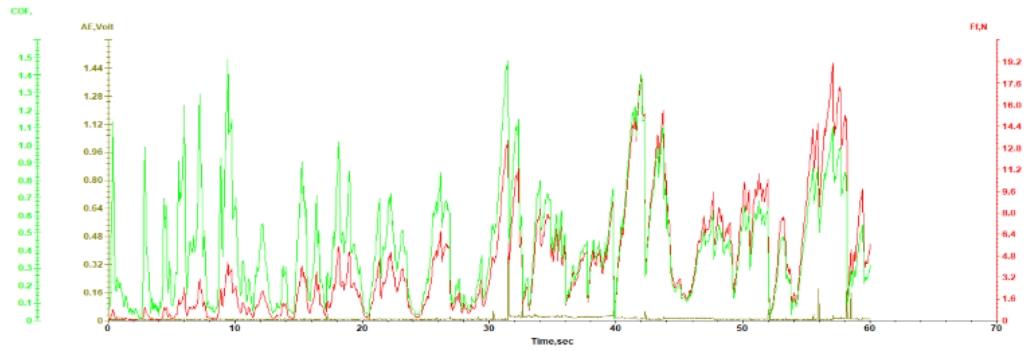

c)

Fig. 5. The time variation diagrams of friction coefficient (COF, green) – friction force (Ff, red) – acoustic emission (AE, brown) for WC-TiC coatings, resulted after the scratch tests with a progressive load of: a) 10 N; b) 15 N; c) 20 N

second a peak of 3N was recorded, in the 20th second a peak of 7 N, higher values between 11-11.5 N were recorded from the 35th second. For the test performed at 20 N a friction force of 4N per second was observed 10, of 6 N in the 22nd second and values between 12-19.2 N starting with the 31st second, the maximum being 19.2 in the 57th second.

Regarding the coefficient of friction, it recorded a behavior similar to that of the friction force in all three cases, with very large variations throughout the test, with an average value of 0.385 and a maximum of 2.5 (second 11) in the test with the load of 10 N, an average value of 0.404 and a maximum of 1.44 (second 35) in the test with the load of 15 N, respectively an average value of 0.425 and a maximum of 1.5 (second 10) at 20 N load.

Another method of characterizing the coatings is the one made with the help of the acoustic emission generated by the tested material during the scratch test, which brings valuable information about the deformations and destruction mechanisms of the tested surfaces. The acoustic emission is presented both in Fig. 5 compared to the friction and COF forces recorded during the scratch tests, but also in Fig. 6, compared to the applied progressive loading force.

In all three cases, it can be observed that the acoustic emission is characterized by only a few peaks, appearing especially after the 30th second, when the applied force exceeds 50%, otherwise an almost linear behavior was recorded, with very small amplitude variations. It should be emphasized that in the case of the test at 20N one can observe (Fig. 6c) the most peaks of acoustic emission (about 11), of high amplitude being the one recorded in the 31st second correlated with a peak of the friction force (see Fig. 5c).

It can be concluded that the structure of the material, formed by a matrix of Fe alloyed with Cr and Ni, hardened with carbides of W and Ti, has a decisive influence on the behavior in the scratch test, represented by a very large variation of the strength

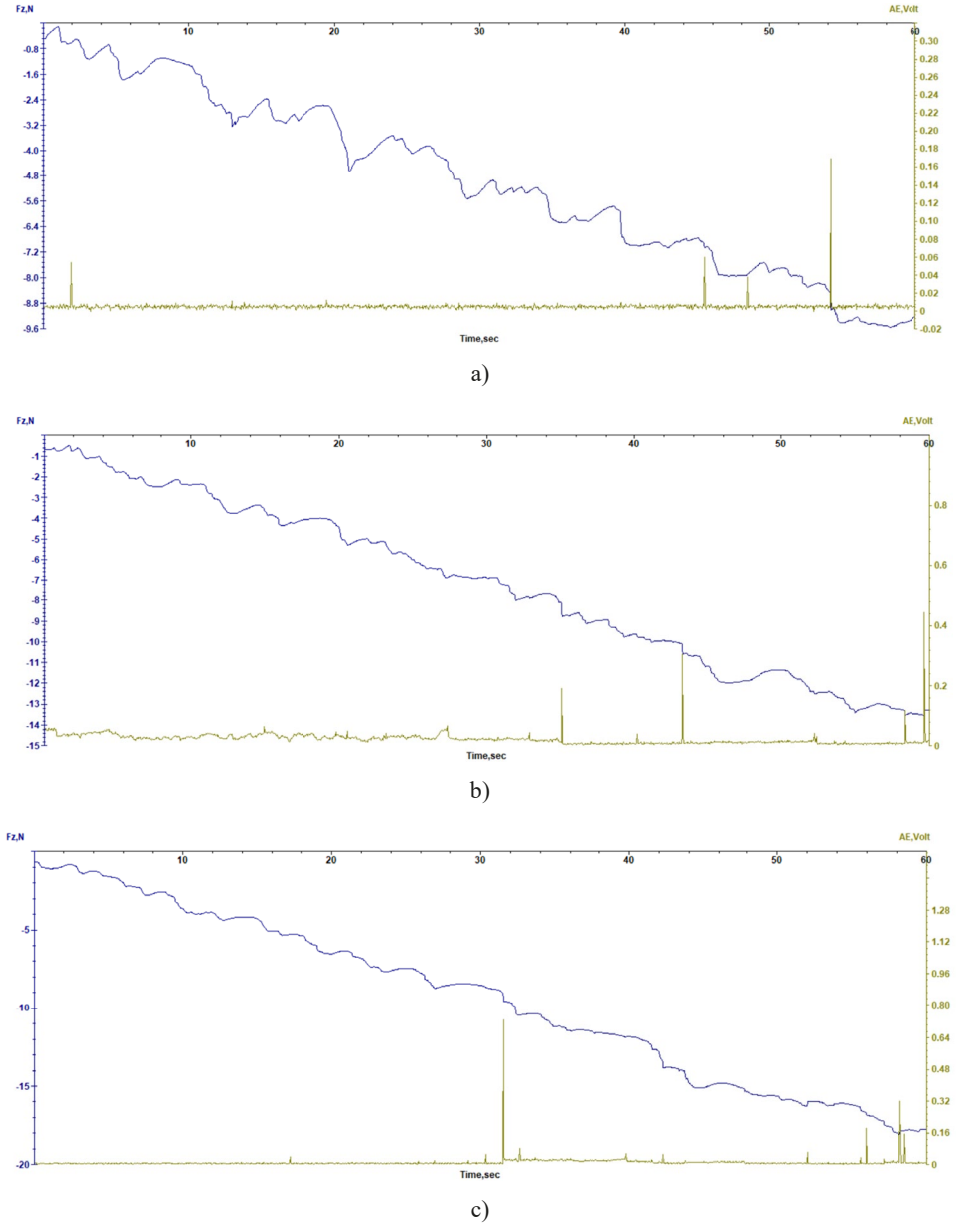

Fig. 6. The time variation diagrams of loading force (Fz, blue) and acoustic emission (AE, brown) for WC-TiC coatings, resulted after the scratch tests with a progressive load of: a) 10 N; b) 15 N; c) 20 N

values friction, respectively of the coefficient of friction. The fact that the matrix takes a large part of the forces applied during the test without allowing cracking or even delamination of the coating is confirmed by the acoustic emission, which does not register many peaks, this behavior also being correlated with the morphological aspect observed through electron microscopy (see Fig. 3) which shows the plastic deformation of the scratch mark without cracking or exfoliation (even partial) of the material in the tested area.

4. Conclusions

Tests have shown that the metal matrix uniformly includes the hard particles arised from the core of the wire, and at the microstructural level, the microhardness varies significantly, depending on the hardness of the particles on which the indentor tip applies the loading forces. However, the overall behavior of the coatings thus realized is a satisfactory one, being, as a general behavior, in the average required by the applications of such a layer.

REFERENCES

[1] A. Tufescu, S. Cretu, M.R. Balan, The role of roughness amplitude on depth distribution of contact stresses. IOP Conference Series: Materials Science and Engineerin **147**, 1 (2016). Article number 012012.

[2] P. Avram, M.S. Imbrea, B. Istrate, S.I. Strugaru, M. Benchea, C. Munteanu, Indian Journal of Engineering and Materials Sciences **21** (3), 315 (2014).

[3] D. Chicet, A. Tufescu, C. Paulin, M. Panturu, C. Munteanu, The Simulation of Point Contact Stress State for APS Coatings. IOP Conference Series: Materials Science and Engineering **209** (1), (2017). Art. number 012044.

[4] J.R. Davis (Ed), Handbook of thermal spray technology, ASM International, Materials Park, OH, USA, 2004.

[5] M. Panturu, D. Chicet, S. Lupescu, B. Istrate, C. Munteanu, Acta Technica Napocensis Series-Applied Mathematics Mechanics and Engineering **61**, 137 (2018).

[6] S. Lupescu, C. Munteanu, A. Tufescu, B. Istrate, N. Basescu, Contact stress simulation problem in case of the Mg alloys. IOP Conference Series: Materials Science and Engineering **997**, 1, (2020). Article number 012024.

[7] L. Pawlowski (Ed.), The Science and Engineering of Thermal Spray Coatings, John Wiley & Sons Ltd, New York (1995).

[8] C. Paulin, D.L. Chicet, B. Istrate, M. Panturu, C. Munteanu, IOP Conference Series: Materials Science and Engineering **147**, 012034 (2016).

[9] W. Tillmann, L. Hagen, D.Stangier, Iris-Aya Laemmerhirt, D. Biermann, P.Kersting, E.Krebs, Wear behavior of bio-inspired and technologically structured HVOF sprayed NiCrBSiFe coatings. Surface & Coatings Technology **280**, 16-26 (2015).

[10] S. L.Toma, et al., Hard Alloys with High Content of WC and TiC- Deposited by Arc Spraying Process, in Welding – Modern Topics, S. C. A. Alfaro, W. Borek, B. Tomiczek (eds.), IntechOpen, London (2020).
DOI: https://doi.org/10.5772/intechopen.94605

[11] V.Goanta, C. Munteanu, S. Müftü, B. Istrate, P. Schwartz, S. Boese, G. Ferguson, C.I. Moraras, Evaluation of the Fatigue Behaviour and Failure Mechanisms of 52100 Steel Coated with WIP-C1 (Ni/CrC) by Cold Spray. Materials **15**, 3609 (2022).
DOI: https://doi.org/10.3390/ma15103609

[12] C.C.Paleu, C. Munteanu, B. Istrate, S. Bhaumik, P. Vizureanu, M.S. Bălţatu, V. Paleu, Microstructural Analysis and Tribological Behavior of AMDRY 1371 (Mo–NiCrFeBSiC) Atmospheric Plasma Spray Deposited Thin Coatings. Coatings **10** (12), 1186 (2020).

[13] P. Sheppard, H. Koiprasert, Effect of W dissolution in NiCrBSi – WC and NiBSi – WC arc sprayed coatings on wear behaviors. Wear **317**, 194-200 (2014).

[14] B. Wielage, H. Pokhmurska, M. Student, V. Gvozdeckii, T. Stupnyckyj, V. Pokhmurskii, Iron-based coatings arc-sprayed with cored wires for applications at elevated temperatures. Surface & Coatings Technology **220**, 27-35 (2013) .

[15] W.Tillmann, L. Hagen, D. Kokalj, Embedment of eutectic tungsten carbides in arc sprayed steel coatings. Surface & Coatings Technology **331**, 153-162 (2017).

[16] W. Tillmann, D.Stangier, Le.Hagen, P. Schröder, M. Krabiell, Influence of theWC grain size on the properties of PVD/HVOF duplex coatings. Surface & Coatings Technology **328**, 326-334 (2017).

[17] A.S. Maxwell, Review of test methods for coating adhesion. 2001, NPL Report MATC (A) 49, National Physical Laboratory, Teddington, Middlesex, UK, ISSN 1473-2734.

[18] W.C. Oliver, G.M. Pharr, Measurement of hardness and elastic modulus by instrumented indentation: Advances in understanding and refinements to methodology. J. Mater. Res. **19**, 1, 3-20 (2004).

[19] Hang Yin, Sheng Wang, Bing Guo, Qingliang Zhao, Effects of scratch depth on material-removal mechanism of yttrium aluminium garnet ceramic. Ceramics International **48**, 27479-27485 (2022).

[20] Ming Liu, Fuwen Yan, Scratch-induced deformation and damage behavior of doped diamond-like carbon films under progressive normal load of Vickers indenter. Thin Solid Films **756**, 139351 (2022).

[21] P. Suya Prem Anand, N. Arunachalam, L. Vijayaraghavan, Evaluation of grinding strategy for bioceramic material through a single grit scratch test using force and acoustic emission signals. Journal of Manufacturing Processes **37**, 457-469 (2019).

[22] R. Ctvrtlík, J. Cech, J. Tomastík, L. Vaclavek, P. Hausild, Plastic instabilities explored via acoustic emission during spherical nanoindentation. Materials Science & Engineering A **841**. 143019 (2022).

[23] R.K. Choudhary, P. Mishra, Use of Acoustic Emission During Scratch Testing for Understanding Adhesion Behavior of Aluminum Nitride Coatings. JMEPEG **25** (6), 2454-2461 (2016).

[24] Antolino Gallego, Jose´ F. Gil, Juan M. Vico, Jose´ E. Ruzzante, Rosa Piotrkowski, Coating adherence in galvanized steel assessed by acoustic emission wavelet analysis. Scripta Materialia **52**, 1069-1074 (2005).

[25] G. Antolino, P. Rosa, R. José, C. Amado, G.U. Teresa, C. Enrique, Acoustic emission technique to assess microfractures of metalic coatings with scratch-tests (2002).
http://www.sea-acustica.es/ PACS.

[26] P. Boháč, J. Tomáštík, R. Čtvrtlík, M. Dráb, V. Koula, K. Cvrk, L. Jastrabík, Acoustic Emission Generated during Scratch Test of Various Thin Films, 11th European Conference on Non-Destructive Testing (ECNDT 2014), Prague 2014, Oct 6-11 (ECNDT 2014) no 16635. http://www.ndt.net/app.ECNDT2014

[27] L. Václavek, J. Tomáštík, H. Chmelícková, R. Ctvrtlík, Benefits of use of acoustic emission in scratch testing. Acta Polytechnica **27** (0), 121-125 (2020).

[28] J. Tomastik, R. Ctvrtlik, P. Bohac, M. Drab, V. Koula, K. Cvrk, L. Jastrabik, Utilization of Acoustic Emission in Scratch Test Evaluation. Key Engineering Materials **662**, 119-122 (2015).